Fortified Astrocyte: The Target of Pathological Intraocular Hypertension

19

Chao Dai, Geoffrey Raisman, and Ying Li

19.1 Gross Anatomy of Rat Optic Nerve Head

The rat optic nerve head (ONH) is a segment about 250 μm in length extending from the funnel-shaped region where the optic nerve fibres (retinal ganglion cell axons, RGC) converge on the optic disc rostrally to the transition to the optic nerve (ON) caudally (Fig. 19.1a). The ONH has a characteristic kidney shape, some 500 μm wide and 300 μm dorsoventrally, with the 'hilus' of the kidney always at the midventral pole and occupied by two large vessels, the ophthalmic vein dorsally and the ophthalmic artery ventral to this (Fig. 19.1b). For complete orientation of the cross sections in space, therefore, it is only necessary to mark the medial and lateral edges at the time when the tissue is removed. The rat ONH contains only three tissue components—totally unmyelinated RGC axons, specialised astrocytes, and the endothelial cells of the microvessels which penetrate from the ventral to the dorsal surfaces (Fig. 19.1d, f, g). Unlike the human lamina cribrosa, there is no connective tissue, collagenous strengthening of the perivascular spaces. Since raised intraocular pressure causes RGC axon damage in the ONH of the rat, this indicates that the injurious effects of pressure transduction can be exerted in the absence of a connective tissue lamina cribrosa (Fig. 19.1c). Both structural integrity and function of axon are supported by astrocytes and microvessels. Astrocytes play the key role in the interactions of axons and microvessels. Rat ONH is a good model to understand the relationship of axon, astrocyte and microvessel in human lamina cribrosa (Fig. 19.1).

19.2 Fortified Astrocytes

The organisation of the ONH consists of a simple radiating array of astrocytes with stout end feet anchored around the midventral, 'hilar' surface facing the ophthalmic vessels (Fig. 19.2a, b). As the astrocytic processes radiate out towards the overarching cap of the dorsal surface, they break up into finer and finer processes, which are either closely apposed to each other or separated by longitudinal channels containing unmyelinated RGC axons (Fig. 19.2a, f, g). The radial processes ultimately terminate in complex delicate branches at the dorsal surface. As they approach the dorsal circumference the radial processes converge into an axon free pre-terminal layer where they branch into fine parallel segments devoid of cytoskeleton and with a tendency to separate (Fig. 19.2c, d).The perinuclear regions of the cell bodies generally lie more or less midway along this trajectory. Longitudinal sections show that the perikarya are packed immediately adjacent to each other in longitudinal rows.

Morphologically the radial astrocytes of the ONH are a unimodal population, the direct descendants of the radial glia of the developing optic stalk. Their ventral, end foot surface is the former pial surface of the optic stalk, and their expanded dorsal circumference is the former ventricular surface which, as in the case of the retina itself, becomes massively expanded. Unlike the retina, however, this former ventricular surface is not fused with an overlying pigment cell layer but is totally denuded of optic stalk cells and apposed directly to a collagen-containing extracellular space. It shows the continuity between this surface and the pigment cell layer of the retina, with the pigment cells ceasing as the ONH is reached.

The ONH astrocytes have a unique cellular composition. In marked contrast to the highly pale cytoplasm of

C. Dai (✉)
Southwest Eye Hospital, Southwest Hospital, Third Military Medical University, Chongqing, China

G. Raisman · Y. Li
UCL Department of Cell and Developmental Biology and Spinal Repair Unit, Department of Brain Repair and Rehabilitation, UCL Institute of Neurology, London, UK

N. Wang (ed.), *Intraocular and Intracranial Pressure Gradient in Glaucoma*,
Advances in Visual Science and Eye Diseases 1, https://doi.org/10.1007/978-981-13-2137-5_19

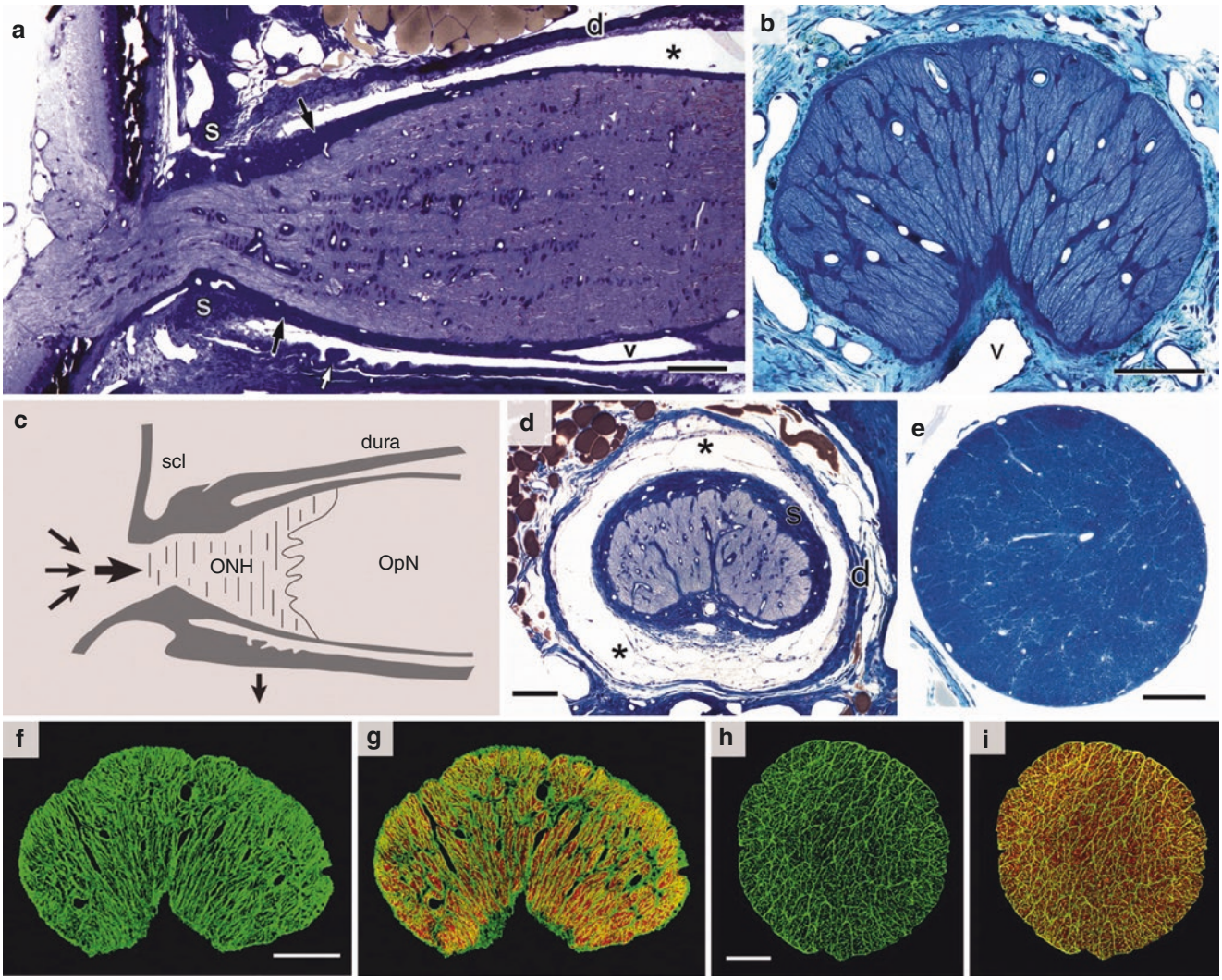

Fig. 19.1 (**a**) Longitudinal section across the ONH from the retina to the junction with the OpN, showing the characteristic longitudinal rows of astrocytic cell bodies. The thick sheath of the ONH (black arrows) is continuous rostrally with the sclera (s) and caudally with the dural sheath of the optic nerve (d). Asterisk, CSF containing subarachnoid space; v, ophthalmic vein; white arrow, arachnoid villus. (**b**) Cross section of ONH showing radial astrocytes and associated microvessels. Stout astrocytic basal processes (stained dark) are anchored on the mid-ventral surface, which is invaginated by the ophthalmic vein (v). (**c**) Line drawing (based on A) showing how the attachments of the thick sheath of the ONH to the sclera (scl) and the dura concentrate the force of raised IOP (arrows) into the ONH at right angles to its radial array of astrocytes. The arachnoid villus (white arrow in Fig. 19.1a above) acts as a drain that would lower the local CSF pressure (down arrow), thus increasing the pressure gradient across the ONH. OpN, optic nerve. (**d**) Cross section showing the thick sheath (s) of the ONH separated by the CSF containing subarachnoid space (*) from the dural sheath (d) of the optic nerve. (**e**–**i**) Cross sections contrasting the ONH (**d**, **f**, **g**) with the OpN (**e**, **h**, i). The ONH has a thick vascular outer sheath and is traversed by darkly stained "fortified" astrocytes that are anchored by thick bases to the deep ventromedian indentation and which radiate out to terminate in thin processes attached to the overarching dorsal surface. The OpN has random arrangement of pale astrocytes and no connective tissue sheath, and the circular outline is not indented. Resin sections (1.5 μm thick) stained with methylene blue and Azur II (**a**, **b**, **d**, **e**). Cryostat sections: GFAP (green) for astrocytes (**f**, **h**), combined with TUJ (red) for axons (**g**, **i**). Scale bars: 100 μm (Reproduced with permission from [1]

astrocytes in virtually every other location (including the retina and the ON) (Fig. 19.2e), the cytoplasm of the ONH astrocytes is highly and uniformly electron dense throughout all the cell processes (Fig. 19.2a, b, i, f). The striking feature of the astrocytic processes is their massive 'strengthening' of longitudinal massed filaments and tubules. We consider this the structural basis of the pressure transduction which gives the ONH its mechanical strength and makes it vulnerable to the distorting effects of raised intraocular pressure (IOP and probably raised CSF pressure). This opinion is supported by our finding that the first effect of raised IOP is a localised tearing away of the fine astrocytic branches from the overlying circumferential surface of the dorsal dome of the ONH. For this reason we refer to these uniquely specialised cells as 'fortified astrocytes (Fig. 19.2).'

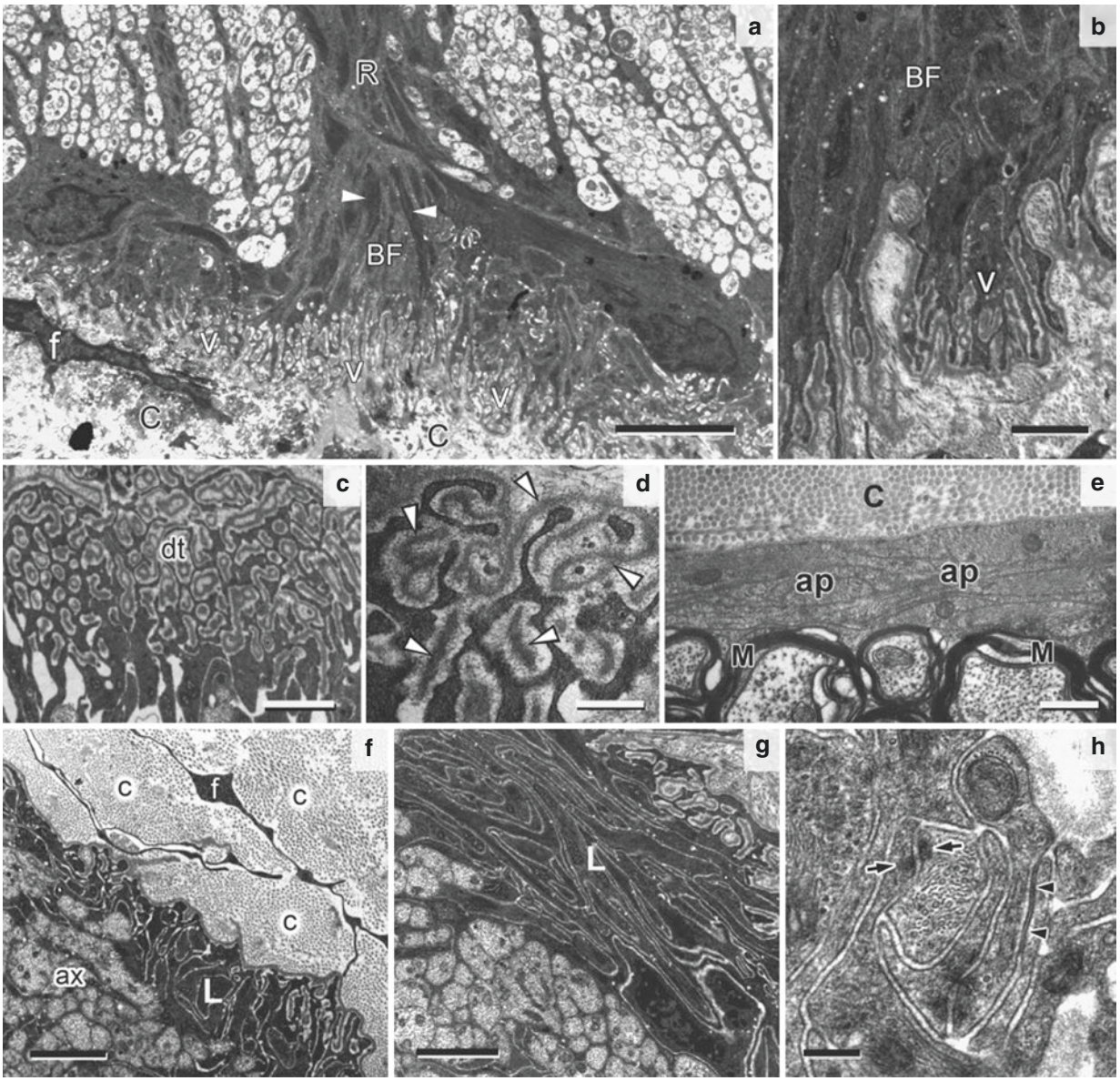

Fig. 19.2 Electron micrographs: (**a**) stout basal foot (BF) of a fortified ONH astrocyte firmly anchored into the collagenous sheath (**c**) by fine, straight villus projections (v) deeply invaginated into the cell cytoplasm. White arrow heads, cytoplasmic swirls of strengthening cytoskeletal filaments and tubules. R, radial processes separated by channels filled with RGC axons; f, fibroblast. (**b**) Enlarged view of astrocytic basal end foot (BF) with straight villi (v) invested with thickened basal lamina. (**c**) Enlarged in (**d**) dorsal terminations of radial glial processes (dt) in a massive cap of complex, interdigitating curved villous processes invested with thickened basal lamina (white arrow heads). (**e**) Segment of the surface of the OpN. In contrast to the ONH where the surface consists of a mass of electron dense villous processes, the surface of the OpN consists of a simple overlay of electron pale astrocytic processes (ap), devoid of villi, and forming the same glia-pial array as found at surface of the rest of the CNS. C, collagen of sheath; M, myelinated RGC axons. (**f**, **g**) The lateral surface of the ONH showing the axon-free region occupied by the electron dense, directly apposed, interweaving preterminal processes (L). Another field at high power in G. ax, axons; collagen (c) and fibroblast (f) of sheath. (**h**) High-power view to show astrocytic junctions: symmetrical desmosome-like (arrows) and gap junction (arrow heads). (**i**) Radial glial process showing aligned cytoskeletal core (f) and fine processes (arrows) arising from the periphery and interweaving among the RGC axons (x). (**j**) Parallel radial array of directly apposed branches of the radial astrocytic process. (**k**) Parallel circumferential array of fibroblasts in the dense collagenous sheath of the ONH. (**l**) Segment of endothelial cell surface from an ONH microvessel, showing the typical array of pinocytotic vesicles on the abluminal surface. In contrast to the OpN (panel M), the endothelial cell is separated from the astrocytic processes (out of the field) by a wide perivascular space containing a fibroblast (fbl) and collagen fibrils. Note that a permeable blood–brain barrier is present in the ONH and absent in the OpN. (**m**) Segment of the surface of an endothelial cell (E) from an OpN microvessel. Note the absence of pinocytotic vesicles and the narrow and uniform apposition (arrows) of the astrocyte (nucleus, n), an anatomical configuration found in regions with a blood–brain barrier. L, lumen. (**n**) Enlarged view of the closely apposed preterminal astrocytic processes (as in **f**, **g**) showing the rich array of pinocytotic vesicles (which may represent a local mechanism to counteract fluid accumulation and close up the spaces during reversible stage of distortion due to mild rises in IOP). See also visible at low power in panels B and J. Scale bars: 5 μm (**a**), 3 μm (**c**), 2.5 μm (**k**), 2 μm (**f**, **g**), 1 μm (**b**, **j**, **m**), 0.5 μm (**d**, **i**, **l**, **n**), 0.2 μm (**e**, **h**) (Reproduced with permission from [1]

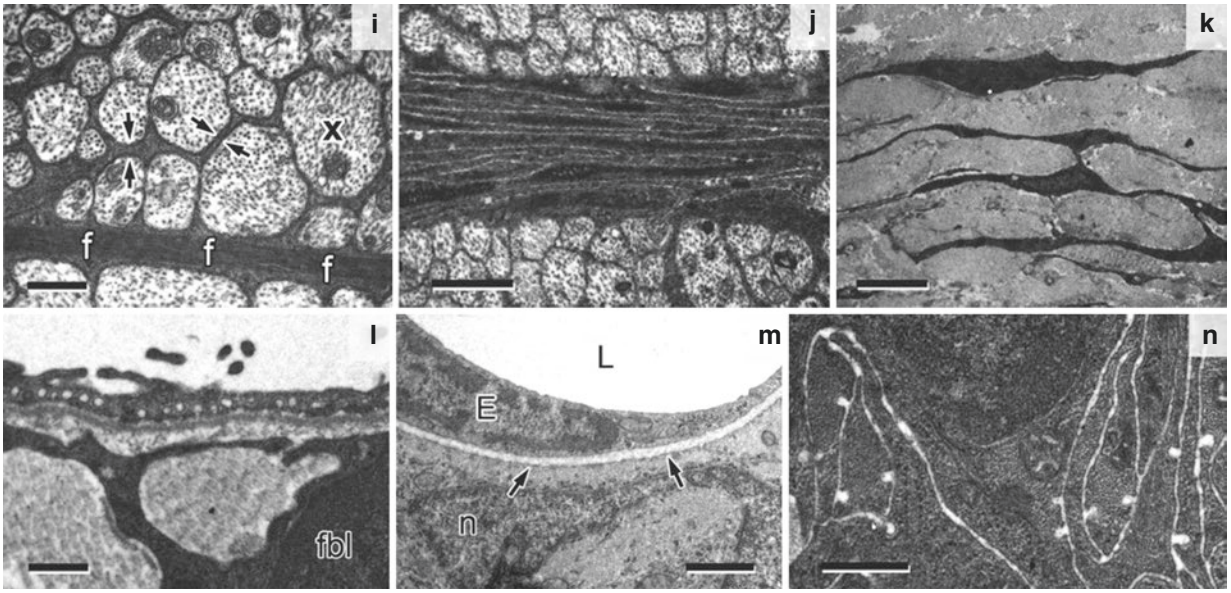

Fig. 19.2 (continued)

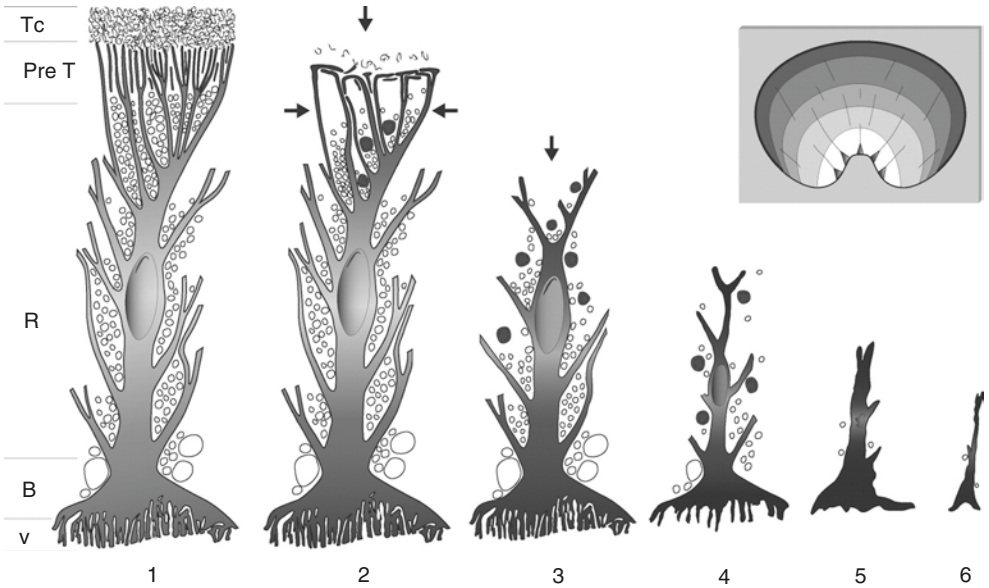

Fig. 19.3 Schematic representation of the changes occurring during damage by raised IOP. (1) Normal structure of a fortified radial astrocyte of the ONH. The enlarged basal end foot (B) is firmly anchored by long, straight villous processes (v) into the collagenous sheath at the ventral median indentation of the ONH. R, radial process branching to enclose separate territories of RGC axons. In the preterminal region (PreT), the finest branches come together in direct apposition to each other and excluding all axons. The terminal cap (TC) is made up of a thick layer of interdigitating curled endings invested with basal lamina. (2) The first stage of damage by raised IOP begins along the dorsal circumference. The preterminal processes become separated by massive spaces of tissue fluid (horizontal arrows). Their terminals are pulled away from the collagenous sheath and collapse (vertical arrow) into reduplicated layers on the dorsal surface. RGC axons spill out into the spaces; degenerating axons (grey-filled circles). The loss of axons is already considerable at this stage. (3)The axon terminals are entirely pulled away (arrow) from the dorsal surface. We suggest this represents the irreversible stage of damage. The space they previously occupied is filled with cellular debris. Axon loss is severe. (4–6) Final stages of degradation leading to loss of all axons and total degeneration of the radial astrocytes. Inset: Isobar representation of stress gradient across the ONH (Reproduced with permission from [1]

19.3 Glial Isomerisation in ONH

At the dorsal surface of the ONH, the radial astrocytic processes branch progressively and lose their cytoskeletal cores of filaments and tubules. This narrow, preterminal region of the ONH (about 1–2 μm deep) is devoid of axons, so that the radial processes converge into direct contact with each other in fine, parallel, electron dense arrays. The preterminal region just under the dorsal surface of the ONH shows a degree of loosening, with spaces filled with extracellular fluid separating the preterminal astrocytic processes (Figs. 19.2c and 19.3), although we have not found any degenerating axons in preterminal area in normal rats with electromicroscopy. The size of space in preterminal region is different in rats and eyeballs with semi-thin sections under light microscopy. Figure 19.4 shows the quite different space in both eyes of one normal rat (Figs. 19.3 and 19.4). There is vulnerable region in the dorsal of ONH. This vulnerable region is isomerisation in bilateral eyes and different rats. The size of space might be related to some vulnerable property. In experimental intraocular hypertension rat, the earliest sign of damage was always seen at the region of the preterminal astrocytic segments just under the dorsal circumferential margin of the ONH (Fig. 19.3).

Glaucoma is the most important cause of irreversible blindness worldwide [2]. A key question in the pathogenesis of glaucoma is to identify the mechanism by pathological high intraocular pressure (IOP). Intraocular hypertension does not always lead to glaucoma. Pathological intraocular hypertension is defined as IOP which could result in glaucoma, even if the IOP is normal. The increased IOP [3–9] or translamina pressure difference (TLPD) [10–14] damages the RGC. What is the first event of the damage procedure? Fortified astrocytes in ONH formed the main supportive structure of glial lamina cribrosa in normal rat. Astrocytes are arranged as a fan-like radial array, firmly attached ventrally to the sheath of the lamina cribrosa by thick basal processes but

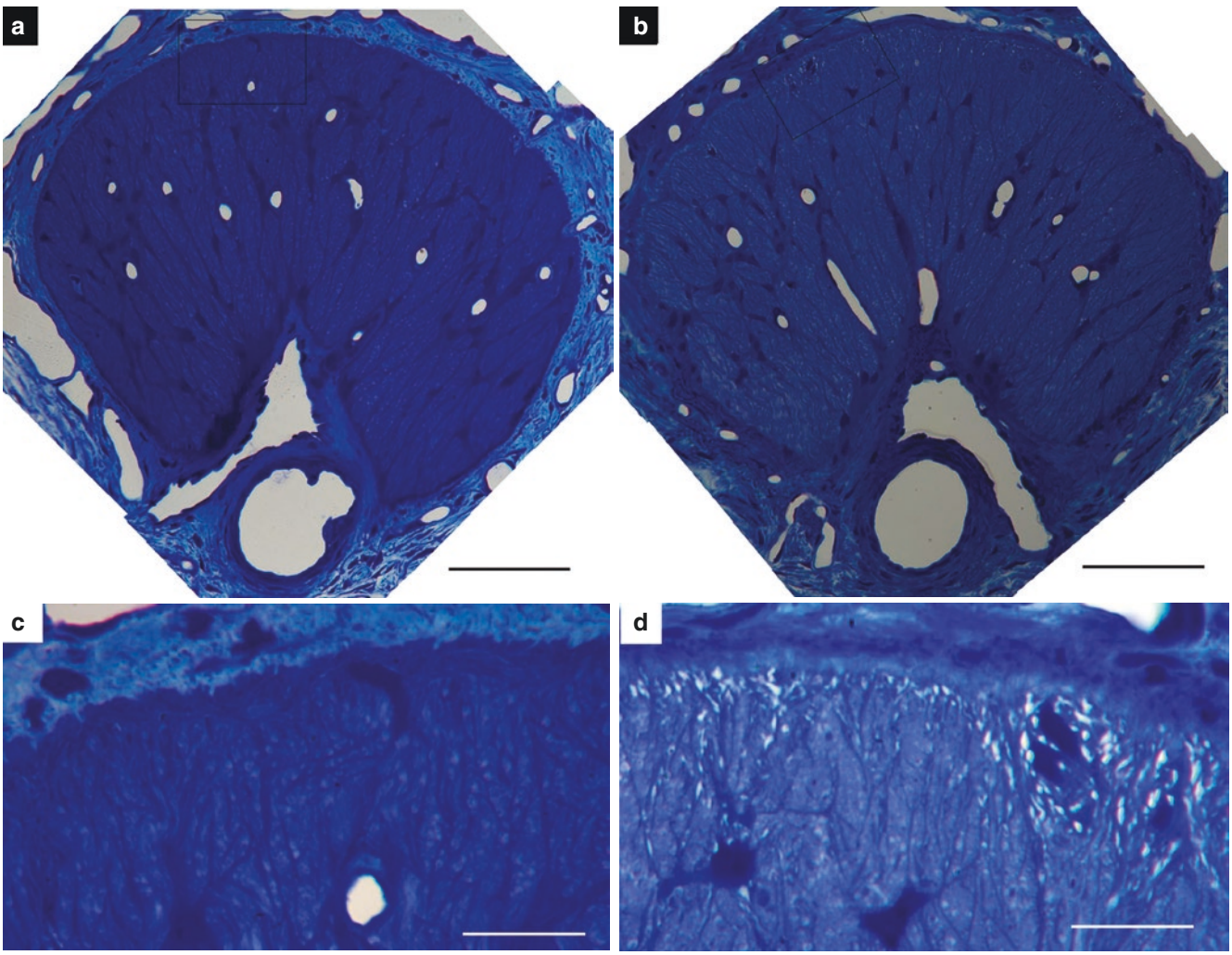

Fig. 19.4 Bilateral ONH of one normal rat. A and C. right ONH, the pre-terminal region is solitary. B and D. left ONH, the pre-terminal region is loosening with obvious space. Scale bars: A-B, 100μm, C-D, 20μm

dividing dorsally into progressively more slender processes with only delicate attachments to the sheath. These fortified astrocytes form ventral stout basal end feet, radial array, and axon-free preterminal layer before terminating in a complex layer of fine interdigitating delicate branches at the dorsal. Fortified astrocyte is highly and uniformly electron dense throughout all the cell processes. An equally striking feature of the astrocytic processes is their massive cytoskeletal 'strengthening' of longitudinal massed filaments and tubules. Especially, cytoskeletal cores form 'scaffold' of astrocytes. There is vulnerable region in the dorsal of glial lamina cribrosa [1, 15]. This vulnerable region is isomerisation in bilateral eyes and different rats. It is hard to test there is also glial isomerisation in human lamina cribrosa. If glial isomerisation also happens in human lamina cribrosa, individual difference of glaucomatous damage may be coincident with glial isomerisation in lamina cribrosa. The deformation of astrocytes in lamina cribrosa could be the 'first event' in glaucomatous optic nerve damage. It hints that glial isomerisation in lamina cribrosa is the mechanism of glaucomatous damage to the optic nerve. With some like solitary preterminal region in lamina cribrosa, intraocular hypertension would not result in RGC damage. On the contrary, with special loosening preterminal region in lamina cribrosa, normal IOP would lead to glaucomatous damage. With increased TLPD or pathological ocular hypertension, the processes of astrocytes withdraw and separate from microvessels, not only focal atrophy will happen, but also blood–brain barrier will be broken. Glaucomatous damage (including optic disc bleeding, immune reaction, ischemia and axon loss of RGC) procedure is set up. With glial isomerisation in ONH, it might throw light on a new hypothesis to understand the mechanism of glaucomatous neuropathy, including mechanical, microcirculatory, immunological, biochemistrical factors. It is owing to the first event of glaucoma, withdrawing processes of fortify astrocytes, which triggers glaucomatous damage.

Acknowledgments The text and figures of this manuscript have appeared previously in our own work: *Dai C, Khaw PT, Yin ZQ, Li D, Raisman G, Li Y. Structural basis of glaucoma: the fortified astrocytes of the optic nerve head are the target of raised intraocular pressure. Glia. 2012;60(1):13–28* [1]. They have been used with permission and edited for this chapter.

References

1. Dai C, Khaw PT, Yin ZQ, Li D, Raisman G, Li Y. Structural basis of glaucoma: the fortified astrocytes of the optic nerve head are the target of raised intraocular pressure. Glia. 2012;60:13–28.
2. Quigley HA, Broman AT. The number of people with glaucoma worldwide in 2010 and 2020. Br J Ophthalmol. 2006;90:262–7.
3. Hernandez MR, Miao H, Lukas T. Astrocytes in glaucomatous optic neuropathy. Prog Brain Res. 2008;173:353–73.
4. Morrison JC, Cepurna Ying Guo WO, Johnson EC. Pathophysiology of human glaucomatous optic nerve damage: insights from rodent models of glaucoma. Exp Eye Res. 2011;93:156–64.
5. Morrison JC, Johnson EC, Cepurna W, Jia L. Understanding mechanisms of pressure-induced optic nerve damage. Prog Retin Eye Res. 2005;24:217–40.
6. Quigley HA, Addicks EM. Regional differences in the structure of the lamina cribrosa and their relation to glaucomatous optic nerve damage. Arch Ophthalmol. 1981;99:137–43.
7. Quigley HA, Addicks EM, Green WR. Optic nerve damage in human glaucoma. III. Quantitative correlation of nerve fiber loss and visual field defect in glaucoma, ischemic neuropathy, papilledema, and toxic neuropathy. Arch Ophthalmol. 1982;100:135–46.
8. Quigley HA, Addicks EM, Green WR, Maumenee AE. Optic nerve damage in human glaucoma. II. The site of injury and susceptibility to damage. Arch Ophthalmol. 1981;99:635–49.
9. Soto I, Oglesby E, Buckingham BP, Son JL, Roberson ED, Steele MR, et al. Retinal ganglion cells downregulate gene expression and lose their axons within the optic nerve head in a mouse glaucoma model. J Neurosci. 2008;28:548–61.
10. Jonas JB, Wang N, Nangia V. Ocular perfusion pressure vs estimated trans-lamina cribrosa pressure difference in glaucoma: The Central India Eye and Medical Study (An American Ophthalmological Society Thesis). Trans Am Ophthalmol Soc. 2015;113:T61–T613.
11. Jonas JB, Wang N, Wang YX, You QS, Yang D, Xie X, et al. Subfoveal choroidal thickness and cerebrospinal fluid pressure: the Beijing Eye Study 2011. Invest Ophthalmol Vis Sci. 2014;55:1292–8.
12. Jonas JB, Wang N, Yang D. Translamina cribrosa pressure difference as potential element in the pathogenesis of glaucomatous optic neuropathy. Asia-Pacific J Ophthalmol. 2016;5:5–10.
13. Zhang Z, Liu D, Jonas JB, Wu S, Kwong JM, Zhang J, et al. Axonal transport in the rat optic nerve following short-term reduction in cerebrospinal fluid pressure or elevation in intraocular pressure. Invest Ophthalmol Vis Sci. 2015;56:4257–66.
14. Zhang Z, Wu S, Jonas JB, Zhang J, Liu K, Lu Q, et al. Dynein, kinesin and morphological changes in optic nerve axons in a rat model with cerebrospinal fluid pressure reduction: the Beijing Intracranial and Intraocular Pressure (iCOP) study. Acta Ophthalmol. 2016;94:266–75.
15. Dai C, Li DQ, Li Y, Raisman G, Yin ZQ. [Studies on glial isomerization of lamina cribrosa in rat], [Zhonghua yan ke za zhi]. Chinese J Ophthalmol. 2013;49:723–8.